Superconductivity in single crystalline Pb nanowires contacted by normal metal electrodes

Jian Wang, Yi Sun, Mingliang Tian, Bangzhi Liu, Meenakshi Singh, and Moses H. W. Chan

Phys. Rev. B **86**, 035439 — Published 24 July 2012

DOI: 10.1103/PhysRevB.86.035439

Superconductivity in single crystalline Pb nanowires contacted by normal metal electrodes

Jian Wang[1,2]*, Yi Sun[1]*, Mingliang Tian[2,3], Bangzhi Liu[4], Meenakshi Singh[2], Moses H. W. Chan[2]*

[1]International Center for Quantum Materials, School of Physics, Peking University, Beijing, 100871, People's Republic of China

[2]The Center for Nanoscale Science and Department of Physics, The Pennsylvania State University, University Park, Pennsylvania 16802-6300, USA

[3]High Magnetic Field Laboratory, Chinese Academy of Science, Hefei 230031, Anhui, People's Republic of China

[4]Materials Research Institute, The Pennsylvania State University, University Park, Pennsylvania 16802-6300, USA

The transport properties of superconducting single crystal Pb nanowires of 55 nm and 70 nm diameter were studied by standard four electrodes method. With normal metal electrodes, resistance-temperature (*R-T*) and magneto-resistance (*R-H*) scans show a series of resistance steps with increasing temperature and magnetic field as the wires are brought toward the normal state. The resistance-current (*R-I*) scans at different temperatures and magnetic fields show that the increase in *R* with *I* is punctuated with sharp steps at specific current values. A large residual resistance is observed down to 2K. The origin of these phenomena is related to the inhomogeneity in the wires and the proximity effect from the normal electrodes.

I. INTRODUCTION

The study of superconductivity in nanowires and quasi-one-dimensional (quasi-1D) nanostructures is driven both by open questions in these systems and their potential applications in dissipationless electronic devices [1-16]. Low dimensional Pb nanostructures have been extensively studied for decades [5-12, 16-18]. Additionally, amorphous and granular nanowires of Pb and other superconducting materials have been studied. [1, 17-21]. In the last few years, there are a number of experiments studying the properties of single crystal superconducting nanowires with diameter less than 100 nm [13,14, 22-24]. An overarching theme of these studies is to understand how superconductivity in these wires is suppressed with decreasing diameter. It is generally accepted that when the diameter of the nanowires is reduced towards and below the Ginzburg-Landau phase coherence length and the magnetic penetration depth [25], the superconductivity is suppressed via thermally activated phase slip [26-28] and quantum phase slip processes [2,3,29,30].

The transport properties of a superconducting nanowire (and indeed any nanowire) is expected to be strongly influenced by the electrodes contacting the wire. The electrode effect on crystalline nanowries has recently been systematically studied. When contacted by superconducting electrodes, normal (Au) [5] and magnetic (Co and Ni) [31] nanowires acquire superconductivity via the proximity effect. A counter intuitive phenomenon known as the anti-proximity was also observed where the superconductivity of thin Zn and Al nanowires was suppressed or weakened when they were contacted by superconducting electrodes [14,23,32]. The effect of normal electrodes on single crystal superconducting nanowires, surprisingly, has not been systematically studied by standard four-probe transport measurements.

In this paper, we report such a study of individual single crystal superconducting Pb nanowires of 55 and 70 nm diameter contacted by four normal Pt electrodes. The diameters of these wires are on the order of the coherence lengths of Pb. Interestingly, *R-T* , *R-H* and *R-I* scans all show a series of resistance steps with increasing temperature, magnetic field, and excitation current respectively as the wires are brought toward the normal state. A large residual resistance is also observed. We attribute these observations to the weakening of superconductivity in the Pb nanowires by the normal Pt electrodes.

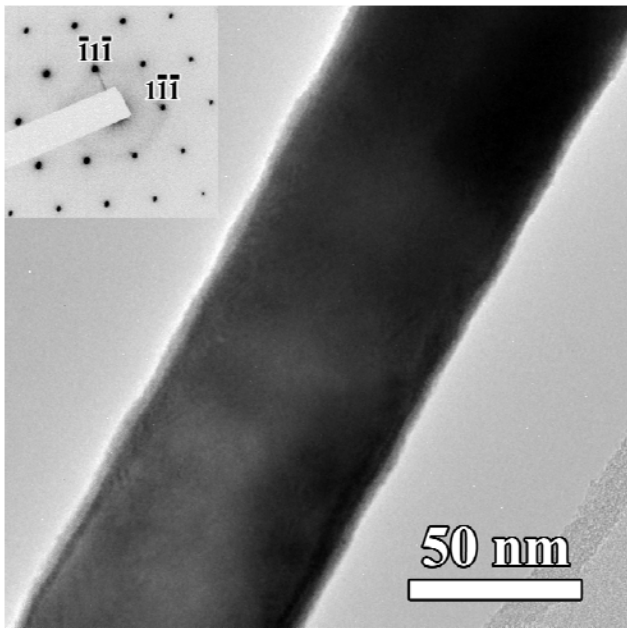

FIG. 1. TEM image of a typical Pb nanowire. The inset shows [110] zone pattern from the same wire.

II. RESULTS and DISCUSSION

The Pb nanowires used in this work were electrodeposited in commercially available track-etched porous polycarbonate membranes that are coated with Au

on one side [13]. The electrolyte $Pb(NH_2SO_3)_2$ was prepared by reacting lead carbonate ($PbCO_3$) with excess sulphamic acid solution in purified H_2O (resistivity>18MΩcm). The transmission electron microscopy (TEM) and selected area electron diffraction study showed that the Pb nanowires were single crystalline (see Fig. 1). A 3-4 nm thick oxide shell surrounding the nanowires was observed, which plays a role in protecting the nanowires from getting damaged during the attachment of the electrodes. Electrical contact to an individual Pb nanowire was made by the following procedure. A drop of the nanowire suspension solution is placed on a silicon substrate with a 1 μm thick Si_3N_4 insulating layer. The sample is then transferred into a focused ion beam (FIB) etching and deposition system (FIB/SEM FEI Quanta 200 3D). Four FIB-assisted Pt strips are deposited onto and make ohmic contact to the Pb nanowire. The deposition current is set to be less than 10 pA to minimize any damage to the nanowire. A scanning electron micrograph of the 55 nm Pb wire contacted in this manner is shown in the inset of Fig. 2a. Transport measurements are carried out in a Physical Property Measurement System cryostat (PPMS-Quantum Design).

Fig. 2 shows the temperature dependence of the electronic transport for the 55 nm and 70 nm diameter nanowires. The distances between two inner edges of the two voltage electrodes of the 70 nm and 55 nm samples were 1.9 μm and 3.7 μm respectively. Figure 2(a) shows *R-T* curve of a 55 nm wire measured with an excitation current of 50 nA from 1.8 K to 300 K at zero magnetic field. The temperature dependence of the resistivities (ρ) of the two wires near and below the superconducting transition temperature *(T_C)* of Pb at different magnetic fields (H) are shown more clearly in Figs. 2(b) and 2(c). The excitation current employed in these measurements is 500 nA. The magnetic field was aligned perpendicular to the nanowires. Two obvious resistance drops at 7.0 K and 4.9 K are seen in the R-T dependence of the 55 nm wire (Fig. 2(b)). For the first step, the resistance decreases by 14% of the normal state value between 6.5 K and 7.0. The resistance drop at the second step at 4.9 K is more gradual. Both steps move to low temperature with increasing field. The wire is normal at an applied field of 20 kOe at 2K. The *ρ-T* curves of 70 nm nanowire (Fig. 2(c)) show three steps at 6.98 K, 5.90 K and 4.67 K. It is reasonable to attribute the resistance drops near 7.0 K found for both wires to the 'intrinsic' superconducting transition of the Pb nanowires since the T_C of bulk Pb is 7.2 K. What then is the origin of the resistance steps well below T_C? According to the TEM images, the nanowire is single crystal and homogeneous. But when the Pt electrodes are deposited onto the nanowires, the FIB fabrication process may introduce inhomogeneity in the contact region. For example the wire in the contact region may become thinner and contaminated by Ga atoms. The characteristic range of the inhomogeneity region is found to be on the order of ~ 190 nm in our samples [33]. This number is reasonable given that the width of the Pt electrodes is on the scale of ~ 190 nm.

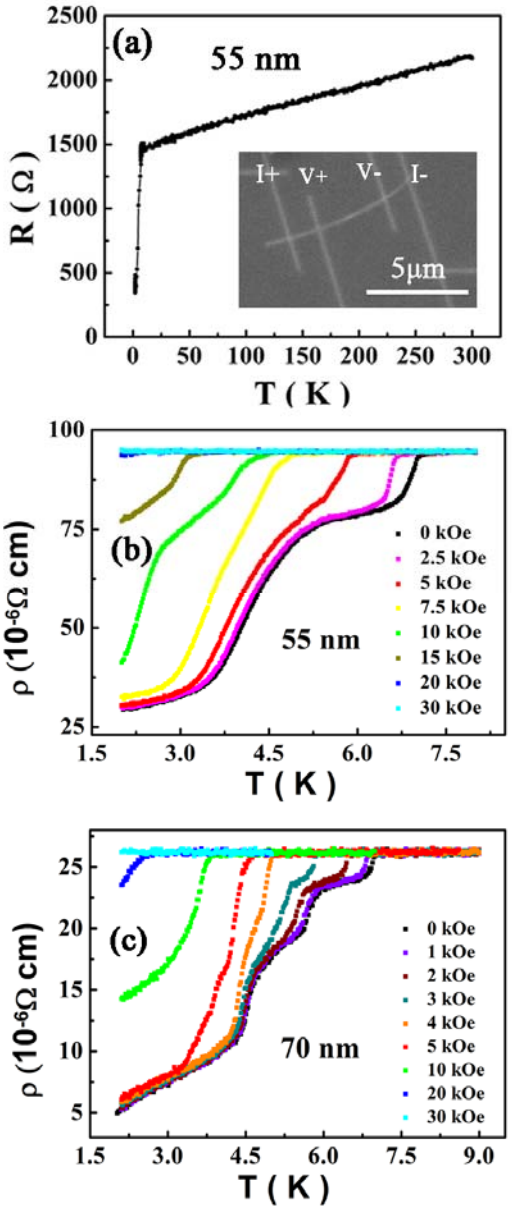

FIG. 2. (Color online) (a) Resistance vs temperature of 55 nm Pb nanowires in the wide temperature range. Inset is the SEM image of the four electrodes measurement; (b) and (c) Resistivity vs temperature of 55 and 70 nm Pb nanowires near and below the T_C in different magnetic fields.

Regular resistance steps in R vs. T curves were reported in micro-scale Sn whiskers (1 μ m × 1 μ m × 1mm) contacted with multiple normal Cu electrodes spaced out along the whisker with the distance between neighboring electrodes ranging from 1.5 μm to 10.5 μm [34]. By making measurements across different electrodes, the authors were able to identify each resistance step as the superconducting transition of a specific section of the whisker. They found the average domain length contributing to each step to be 20-900 nm. The observed steps are attributed to the effect of the normal metal electrodes on the superconductor [34]. The resistance

steps found here at temperature well below 7K may have the same origin as that found in ref. 34. However, in our situation, a finite resistance of 20% and 30% of the normal state resistance is found down to 2K. This is unlikely to be due to the inhomogeneity in the wire since the inhomogeneity extends only ~190 nm out of a total length of 1.9 μm and 3.7 μm.

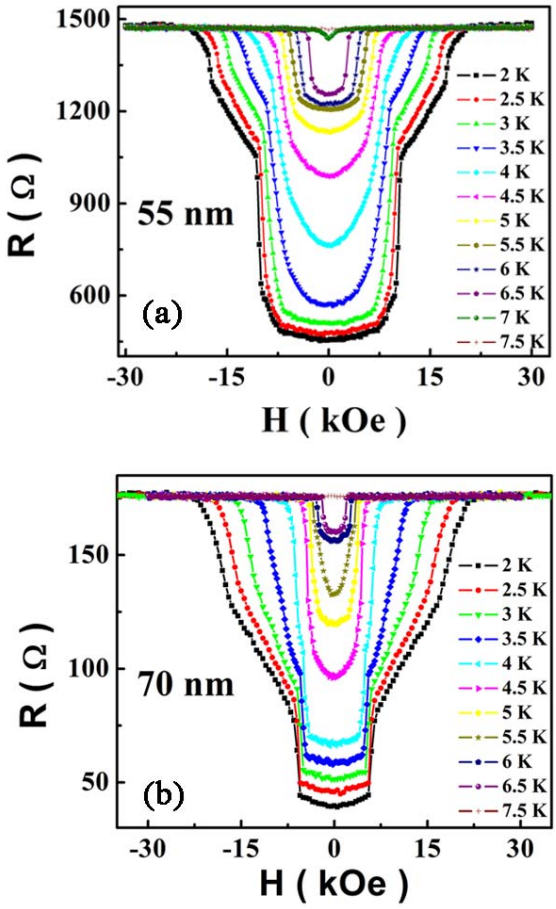

FIG. 3. (Color online) Magnetoresistance *vs* magnetic field of 55 and 70 nm Pb nanowires at different temperatures.

The normal Pt electrodes are expected to have a "reversed" proximity effect on the superconducting Pb nanowires. This effect will weaken the superconductivity of the Pb nanowires and may account for the residual resistance at temperatures well below T_C of Pb. If the residual resistance is indeed due to this 'reversed' proximity effect, the range of this effect can be estimated to be around 180 and 550 nm for the 70 nm and 55 nm nanowire respectively. This range is consistent with the range of the regular proximity effect induced by superconducting electrodes on a normal nanowire [5]. The resistivities of the 70 nm and 55 nm Pb nanowires at room temperature are 26×10^{-6} Ω cm and 94×10^{-6} Ω cm respectively. These numbers are on the same order as the resistivity of bulk Pb (21.3×10^{-6} Ω cm). The larger ρ of the thinner wire is probably the effect of enhanced surface scattering. We note that in our four-probe measurement configuration, the contact resistance can be neglected.

Figure 3 shows the resistance of the Pb nanowires as a function of the magnetic field (H) perpendicular to the nanowires at different temperatures. The excitation current is 500 nA for 55 nm wire and 1 μA for 70 nm wire. Sharp and well defined resistance steps are found in R vs. H scans at low temperature (Fig. 3a and Fig. 3b). The first step was found near 10 kOe for the 55 nm wire and 7.2 kOe for the 70 nm wire. The magnitudes of the resistance steps in the *R-H* scans at different temperatures are consistent with the steps found in the *R-T* scans at different field values. Substantial residual resistances near zero field at low temperature are clearly displayed. The field at which the two wires are driven into the normal state are almost same (21 kOe) but much larger than that of the bulk Pb (0.803 kOe at zero temperature, 0.74 kOe at 2.0 K). This enhancement in the critical field is a well-studied phenomenon in nanoscale superconductors [35]. With increasing temperature, the critical field decreases and the steps become less well defined and rounded.

The *R-I* curves of the two Pb nanowires measured at different temperatures under zero field are shown in Figs. 4(a) and 4(c), the measurement under different perpendicular magnetic fields at 2 K are shown in Figs. 4(b) and 4(d). The corresponding *V-I* scans at zero field at different temperatures and the *V-I* scans at different fields at 2K of the 70 nm wire are shown in Fig. 4(e) and Fig. 4(f) Similar dependences on the excitation current are found in the two wires. The increase in resistance and voltage with increasing current is punctuated by sharp steps. Fig. 4(d) shows that the resistance of 70 nm wire at 2 K reaches almost zero in the low current limit of our measurement at 50 nA, but the 55 nm sample (in Fig. 4(b)) shows a residual resistance of about 10^2 Ω. Unfortunately, we were limited by our equipment and measurement noise from extending the measurement to lower current and temperature. The normal state resistance of 180 Ω of the 70 nm wire at 2K and zero field is reached with stepwise increase in resistance at 50 nA, 5.40 μA, 9.47μA, 13.00 μA, and 25.47 μA. At higher temperatures, the first step is no longer found and the other steps move to lower current values. Under a field of 2.5 kOe at 2K, the resistance steps also move to lower current values (Fig. 4(d)). Similar dependence of these 'critical' current like resistance steps on temperature and magnetic field have been reported in superconducting whiskers [36,37], microbridges [38], and nanowires[13,23,39-41]. The observed *V-I* steps are

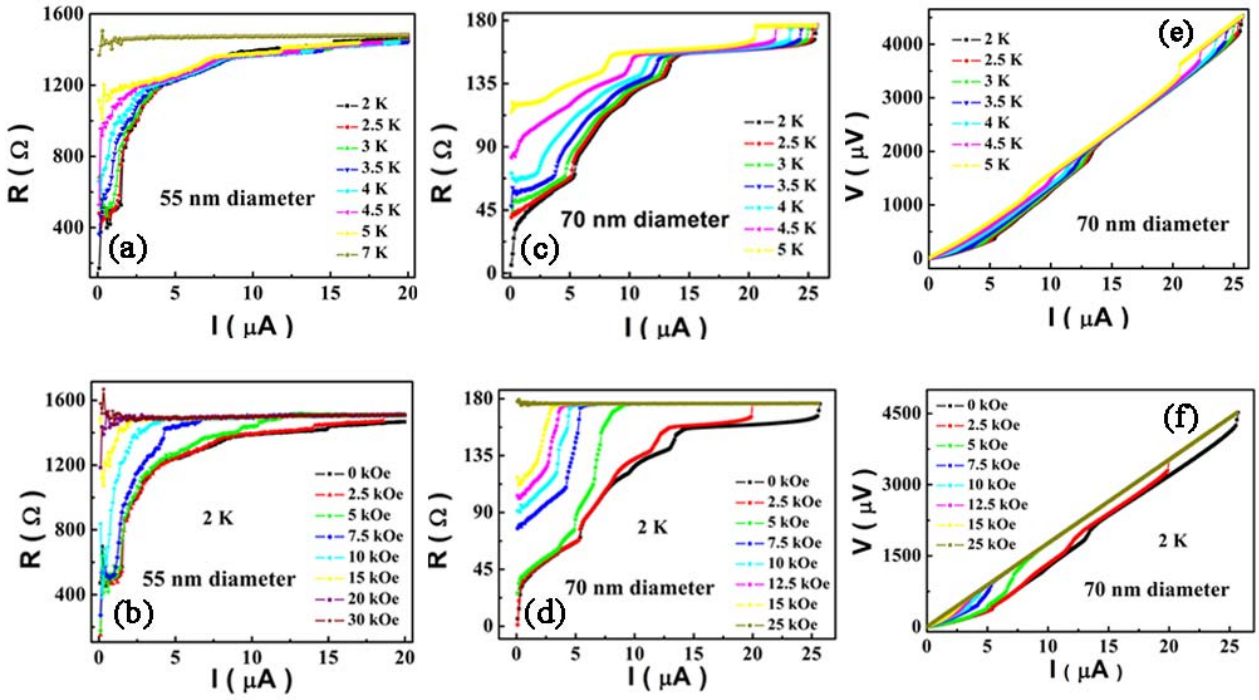

FIG. 4. (Color online) Resistance vs current of 55 and 70 nm Pb nanowires at different temperatures [(a) and (c)] and in different magnetic fields [(b) and (d)]. (e) and (f): voltage vs current curves of 70 nm Pb nanowires at different temperatures and magnetic fields.

reminiscent of phase slip centers (PSCs) behavior. However, there are some differences between the conventional PSCs and our observations. In experiments that display standard PSC behavior, true zero resistance state is found below a certain threshold bias current. With increasing current, the resistance increases with uniform steps above this threshold current. In our situation the resistance steps are not uniform and in the case of the 55 nm wire, a large residual resistance is found even at the lowest excitation current. The residual resistance, as explained before, is a consequence of the 'reverse' proximity effect. The nonuniformity of the steps might be a consequence of the inhomogeneity introduced in the Pb wires during FIB assisted deposition of the Pt electrodes. The inhomogeneity introduced by the electrodes may not have played an important role in the earlier studies of PSCs since the length of the wires was relatively long or the electrode deposition process was less invasive.

III. CONCLUSIONS

In summary, single crystal Pb nanowires of two different diameters were fabricated by electrochemical deposition. *R-T*, *R-H* and *R-I* curves measured by standard four-probe configuration show a series of resistance steps with increasing temperature, magnetic field, and excitation current. Residual resistances are also observed under T_C. We attribute these phenomena to inhomogeneity in the wire and proximity effect introduced by the normal metal (Pt) electrodes.

ACKNOWLEDGMENT

This work was financially supported by the Penn State MRSEC under NSF grant DMR-0820404, National Basic Research Program (NBRP) of China (No. 2012CB921300), the National Natural Science Foundation of China (No. 11174007), the National Key Basic Research of China under Grant No. 2011CBA00111 and China Postdoctoral Science Foundation (No. 2011M500180).

* jianwangphysics@pku.edu.cn (Wang);
yisun@pku.edu.cn (Sun);
chan@phys.psu.edu (Chan).

[1] A. Bezryadin, C. N. Lau, and M. Tinkham, Nature (London) **404**, 971 (2000).

[2] K. Y. Arutyunov, D. S. Golubev, and A. D. Zaikin, Phys. Rep. **464**, 1 (2008).

[3] D. S. Golubev and A. D. Zaikin, Phys. Rev. B **64**, 014504 (2001).

[4] N. Giordano, Phys. Rev. Lett. **61**, 2137 (1988).

[5] J. Wang, C. T. Shi, M. L. Tian, Q. Zhang, N. Kumar, J. K. Jain, T. E. Mallouk, and M. H. W. Chan, Phys. Rev. Lett. **102**, 247003 (2009).

[6] J. Wang, X. C. Ma, L. Lu, A. Z. Jin, C. Z. Gu, X. C. Xie, J. F. Jia, X. Chen, and Q. K. Xue, Appl. Phys. Lett. **92**, 233119 (2008).

[7] J. Wang, X. C. Ma, Y. Qi, Y. S. Fu, S. H. Ji, L. Lu, J. F. Jia, and Q. K. Xue, Appl. Phys. Lett. **90**, 113109 (2007).

[8] J. Wang, X. C. Ma, Y. Qi, Y. S. Fu, S. H. Ji, L. Lu, A. Z. Jin, C. Z. Gu, X. C. Xie, M. L. Tian, J. F. Jia, and Q. K. Xue, J. Appl. Phys. **106**, 034301 (2009).

[9] J. Wang, J. F. Jia, X. C. Ma, Q. T. Shen, T. Z. Han, A. Z. Jin, L. Lu, C. Z. Gu, M. L. Tian, X. C. Xie, X. Chen, and Q. K. Xue, J. Vac. Sci. Technol. B **28**, 678 (2010).

[10] J. Wang, X. C. Ma, S. H. Ji, Y. Qi, Y. S. Fu, A. Z. Jin, L. Lu, C. Z. Gu, X. C. Xie, M. L. Tian, J. F. Jia, and Q. K. Xue, Nano Res. **2**, 671 (2009).
[11] J. Wang, X. C. Ma, Y. Qi, Y. S. Fu, S. H. Ji, L. Lu, X. C. Xie, J. F. Jia, X. Chen, and Q. K. Xue, Nanotechnology **19**, 475708 (2008).
[12] Z. L. Guan, Y. X. Ning, C. L. Song, J, Wang, J. F. Jia, X. Chen, Q. K. Xue, and X. C. Ma, Phys. Rev. B **81**, 054516 (2010).
[13] M. L. Tian, J. G. Wang, J. S. Kurtz, Y. Liu, and M. H. W. Chan, Phys. Rev. B **71**, 104521 (2005).
[14] M. L. Tian, N. Kumar, S. Y. Xu, J. G. Wang, J. S. Kurtz, and M. H. W. Chan, Phys. Rev. Lett. **95**, 076802 (2005).
[15] J. Hua, Z. L. Xiao, A. Imre, S. H. Yu, U. Patel, L. E. Ocola, R. Divan, A. Koshelev, J. Pearson, U. Welp, and W. K. Kwok, Phys. Rev. Lett. **101**, 077003 (2008).
[16] Y. Guo, Y. F. Zhang, X. Y. Bao, T. Z. Han, Z. Tang, L. X. Zhang, W. G. Zhu, E. G. Wang, Q. Niu, Z. Q. Qiu, J. F. Jia, Z. X. Zhao, and Q. K. Xue, Science **306**, 1915 (2004).
[17] P. Xiong, A. V. Herzog, and R. C. Dynes, Phys. Rev. Lett. **78**, 927 (1997).
[18] A. V. Herzog, P. Xiong, F. Sharifi, and R. C. Dynes, Phys. Rev. Lett. **76**, 668 (1996).
[19] S. Michotte, S. Mátéfi-Tempfli and L. Piraux, Appl. Phys. Lett. **82**, 4119 (2003).
[20] S. Michotte, S. Mátéfi-Tempfli and L. Piraux, Supercond. Sci. Technol. **16**, 557 (2003).
[21] F. Altomare, A. M. Chang, M. R. Melloch, Y. G. Hong, and C. W. Tu, Phys. Rev. Lett. **97**, 017001 (2006).
[22] M. L. Tian, J. G. Wang, N. Kumar, T. H. Han, Y. Kobayashi, Y. Liu, T. E. Mallouk and M. H. W. Chan, Nano Lett. **6**, 2773 (2006).
[23] M. L. Tian, N. Kumar, J. G. Wang, S. Y. Xu, and M. H. W. Chan, Phys. Rev. B **74**, 014515 (2006).
[24] H. D. Liu, Z. X. Ye, Z. P. Luo, K. D. D. Rathnayaka, and W. H. Wu. Physica C **468**, 304 (2008).
[25] W. J. Skocpol, M. Tinkham, Rep. Prog. Phys. **38**, 1049 (1975).
[26] W. A. Little, Phys. Rev. **156**, 396 (1967).
[27] J. S. Langer and V. Ambegaokar, Phys. Rev. **164**, 498 (1967).
[28] D. E. McCumber and B. I. Halperin, Phys. Rev. B, **1**, 1054 (1970).
[29] A. D. Zaikin, D. S. Golubev, A. van Otterlo, G. T. Zimanyi, Phys. Rev. Lett. **78**, 1552 (1997).
[30] J. M. Duan, Phys. Rev. Lett. **74**, 5128 (1995).
[31] J. Wang, M. Singh, M. L. Tian, N. Kumar, B. Z. Liu, C. T. Shi, J. K. Jain, N. Samarth, T. E. Mallouk and M. H. W. Chan, Nature Phys. **6**, 389 (2010).
[32] M. Singh, J. Wang, M. L. Tian, T. E. Mallouk and M. H. W. Chan, Phys. Rev. B, **83**, 220506 (2011).
[33] K. Yu. Arutyunov, D. A. Presnov, S. V. Lotkhov, A. B. Pavolotski and L. Rinderer, Phys. Rev. B, **59**, 6487 (1999).
[34] K. Yu. Arutyunov, T. V. Ryynänen, J. P. Pekola and A. B. Pavolotski, Phys. Rev. B, **63**, 092506 (2001).
[35] S. Dubois, A. Michel, J. P. Eymery, J. L. Duvail and L. Piraux, J. Mater. Res., **14**, 665 (1999).
[36] J. Meyer and G. V. Minniger, Phys. Lett. **38**, 529 (1972).
[37] U. Schulz and R. Tidecks, Solid State Communications, **57**, 829 (1986).
[38] W. J. Skocpol, M. R. Beasley, and M. Tinkham, J. Low Temp. Phys. 16, 145 (1974).
[39] D. Y. Vodolazov, F. M. Peeters, L. Piraux, S. Mátéfi-Tempfli, and S. Michotte, Phys. Rev. Lett. **91**, 157001 (2003).
[40] D. Lucot, F. Pierre, D. Mailly, K. Yu-Zhang, S. Michotte, F. de Menten de Horne, and L. Piraux, Appl. Phys. Lett. **91**, 042502 (2007).
[41] H. D. Liu, Z. X. Ye, W. H. Wu, and K. D. D. Rathnayaka, J. Appl. Phys. **105**, 07E305 (2009).